Available online at www.sciencedirect.com
ScienceDirect
Nuclear Instruments and Methods in Physics Research A 569 (2006) 350–354
NUCLEAR INSTRUMENTS & METHODS IN PHYSICS RESEARCH Section A
www.elsevier.com/locate/nima

Comparative study using Monte Carlo methods of the radiation detection efficiency of LSO, LuAP, GSO and YAP scintillators for use in positron emission imaging (PET)

Dimitrios Nikolopoulos[a], Ioannis Kandarakis[a,*], Xenophon Tsantilas[b], Ioannis Valais[a], Dionisios Cavouras[a], Anna Louizi[b]

[a]*Department of Medical Instruments Technology, Technological Educational Institution of Athens, Ag. Spiridonos 12210, Athens, Greece*
[b]*Department of Medical Physics, University of Athens, Athens, Greece*

Available online 8 September 2006

Abstract

The radiation detection efficiency of four scintillators employed, or designed to be employed, in positron emission imaging (PET) was evaluated as a function of the crystal thickness by applying Monte Carlo Methods. The scintillators studied were the $LuSiO_5$ (LSO), $LuAlO_3$ (LuAP), Gd_2SiO_5 (GSO) and the $YAlO_3$ (YAP). Crystal thicknesses ranged from 0 to 50 mm. The study was performed via a previously generated photon transport Monte Carlo code. All photon track and energy histories were recorded and the energy transferred or absorbed in the scintillator medium was calculated together with the energy redistributed and retransported as secondary characteristic fluorescence radiation. Various parameters were calculated e.g. the fraction of the incident photon energy absorbed, transmitted or redistributed as fluorescence radiation, the scatter to primary ratio, the photon and energy distribution within each scintillator block etc. As being most significant, the fraction of the incident photon energy absorbed was found to increase with increasing crystal thickness tending to form a plateau above the 30 mm thickness. For LSO, LuAP, GSO and YAP scintillators, respectively, this fraction had the value of 44.8, 36.9 and 45.7% at the 10 mm thickness and 96.4, 93.2 and 96.9% at the 50 mm thickness. Within the plateau area approximately (57–59)%, (59–63)%, (52–63)% and (58–61)% of this fraction was due to scattered and reabsorbed radiation for the LSO, GSO, YAP and LuAP scintillators, respectively. In all cases, a negligible fraction (<0.1%) of the absorbed energy was found to escape the crystal as fluorescence radiation.

Keywords: Scintillators; PET imaging; Monte Carlo; Radiation detectors

1. Introduction

Positron emission tomography (PET) is a very powerful medical diagnostic method to observe the metabolism, blood flow, neurotransmission and handling of important biochemical entities [1]. Among the various scintillators employed in detector geometries present at commercial PET systems, $Be_4Ge_3O_{12}$ (BGO) is the one most frequently used [1]. Yet, there is a growing interest in introducing new scintillator materials (Table 1) mainly due to the fact that other properties of BGO, such as its light yield, energy resolution and response time, make it less optimal for application in PET [1]. LSO:Ce is the most important competitor for replacing BGO, especially in recently developed hybrid PET/CT systems [1–3], mainly due to its high detection efficiency. This scintillator is also reported to be used in small-animal PET systems [1] as well as in PET/mammography systems [1,4]. GSO:Ce is currently used in whole body PET/CT systems and it has not only been used in brain PET. [5]. Furthermore, several other small animal PET systems have been developed by application of the relatively low density, small-Z scintillator $YAlO_3$:Ce (YAP:Ce) [6,7]. In addition, $LuAlO_3$:Ce (LuAP:Ce) could also be considered as a very interesting candidate to replace BGO in PET because its light yield is higher and the response time is much faster than those of BGO [1].

*Corresponding author. Tel.: +30 210 5385387; fax: +30 210 5385302.
E-mail address: kandarakis@teiath.gr (I. Kandarakis).

0168-9002/$ - see front matter © 2006 Elsevier B.V. All rights reserved.
doi:10.1016/j.nima.2006.08.033

Table 1
Characteristics of the scintillators considered

Scintillator	Density ($g\,cm^{-3}$)	$\rho\ Z_{eff}^4$ (10^4)	Light yield (photons/MeV)
LSO	7.4	143	26 000
LuAP	8.3	148	12 000
GSO	6.7	84	8000
YAP	5.5	7	21 000

The purpose of this paper was the investigation of the absorption properties and the radiation detection efficiency of the $LuSiO_5$ (LSO), Gd_2SiO_5 (GSO), $YAlO_3$ (YAP) and $LuAlO_3$ (LuAP) scintillator for possible applications in PET systems by Monte Carlo methods. The scintillator absorption properties were studied as a function of crystal thickness.

2. Materials and methods

2.1. Brief description of the Monte Carlo code

The Monte Carlo codes previously generated by the reporting team [8] were properly modified so as to be efficient for PET and easily adjustable to various scintillator materials. Photon transport modelling was based on methods proposed by Chan and Doi [9,10] by making use of the basic photon interaction mechanisms at 511 keV, as well as the form and scatter factors of the materials under study. The cross sections of the scintillator materials were calculated using the XCOM code (NIST) [11], in accordance to tabulation of Hubbell and Seltzer [12]. The form factors and the scatter factors of the scintillator materials were calculated from those corresponding to the elements constituting these scintillator materials using specially designed codes. The factors for the elements were downloaded from the NIST reference database [13]. K- or L-characteristic quanta were modelled independently as photons initiating their history at the photoelectric interaction site. Various Monte Carlo simulation runs were performed. In every run 10^7 photons were generated and tracked. All photon track and energy histories were recorded for further analysis.

2.2. Detector parameters studied

The detector parameters studied, were the efficiency of absorption of incident energy (EAIE) the quantum detection efficiency (QDE) and the quantum absorption efficiency (QAE) [14]. The EAIE was defined as the fraction of the totally absorbed photon energy over the total incident energy [15]. The EAIE was classified into two classes: (a) overall absorbed-EAIE: energy absorbed due to all types of absorption mechanisms i.e. photoelectrons ejected after a photoelectric effect, electrons ejected after a Compton event, and Auger electrons ejected after X-ray fluorescence transitions following a photoelectric effect. (b) Scattered and reabsorbed-EAIE: energy absorbed after one or multiple scattering events of the primary photons. QDE and QAE were defined as the number of the detected and totally absorbed photons respectively over the total number of incident photons [15]. QAE was accompanied by an additional class; QAE-photoelectrically absorbed (QAE-PA); via one-hit photoelectric event.

2.3. Simulated detector exposures

The scintillators were modelled as blocks of various coating thicknesses. A series of thicknesses ranging from 0 to 50 mm were investigated. Detector parameters studied, were investigated at 511 keV constant photon energy.

Modelled scintillators were considered to be exposed to gamma rays initiating from a point source located at the central axis of the entrance area of the scintillator block at pencil beam geometry. This exposure geometry was arbitrarily considered to correspond to the one of two annihilation quanta that collinearly hit the centres of two detectors of a PET system.

3. Results and discussion

Fig. 1 presents the overall absorbed-EAIE and Fig. 2 the scatter and reabsorbed-EAIE, which is produced as a result of X-ray energy deposition within the scintillator.

The overall absorbed-EAIE at 511 keV of the LSO, GSO and LuAP crystals was found to increase with increasing crystal thickness tending to form a plateau above the 40 mm thickness. For these crystals this EAIE at the 10 mm thickness had the values of 44.8%, 36.9% and 45.7%, respectively, and 96.4%, 93.2% and 96.9% at the 50 mm thickness. On the other hand, the overall absorbed-EAIE of the YAP crystals was found to increase continuously in the whole of the examined thickness range, i.e. from 0 to 50 mm. The overall absorbed-EAIE of the YAP crystals presented the values of 16.8% at the 10 mm crystal

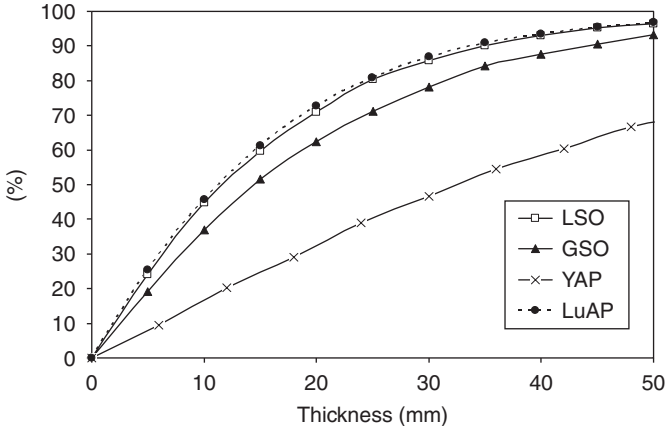

Fig. 1. Overall absorbed-EAIE at 511 keV for the four scintillators under study.

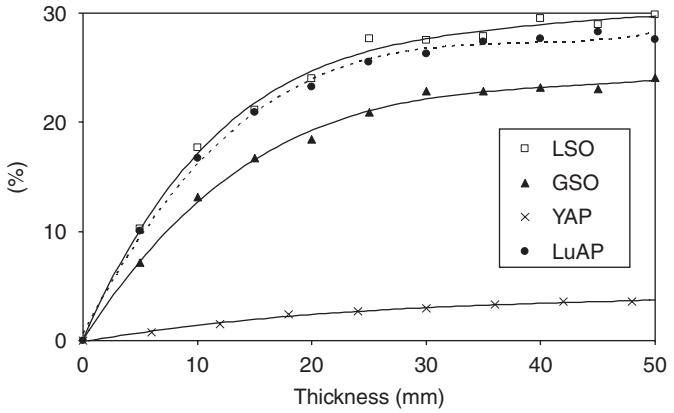

Fig. 2. Scatter and reabsorbed-EAIE at 511 keV for the four scintillators under study.

thickness and 68.1% at the 50 mm thickness, respectively. These results are within the range reported by a recent review paper of van Eijk [1].

The remaining part of the overall absorbed-EAIE corresponds to the fraction of the total energy that escapes the crystal, i.e. energy lost. This fraction, more or less, is an additional indicator of the crystal's ability to capture useful signal—true coincidences. For the LSO scintillator this fraction was calculated to be 77.1% at the 10 mm thickness and 3.85% at the 50 mm thickness. For the GSO scintillator these values were found equal to 82.4% and 7.21%, for the YAP scintillator 83.2 and 31.9% and for the LuAP scintillator, 75.8% and 2.97%, respectively.

The remaining part of the overall absorbed-EAIE corresponds to the fraction of the total energy that escapes the crystal, i.e. energy lost. This fraction, more or less, is an additional indicator of the crystal's ability to capture useful signal—true coincidences. For the LSO scintillator this fraction was calculated to be 77.1% at the 10 mm thickness and 3.85% at the 50 mm thickness. For the GSO scintillator these values were found equal to 82.4% and 7.21%, for the YAP scintillator 83.2% and 31.9% and for the LuAP scintillator 75.8 and 2.97%, respectively.

At the thickness range studied, scatter and reabsorbed-EAIE was found to present similar curve shape to that of the overall absorbed-EAIE for all scintillators studied. Generally, the scatter and reabsorbed-EAIE increases with crystal thickness. For the LSO crystals this EAIE had the values of 12.8% at the 10 mm thickness and 59.9% at the 50 mm thickness. For the GSO crystals these values were 22.3% and 63.5%, whereas for the YAP and LuAP crystals 15.2% and 62.9%, and 26.2% and 61.6%, respectively. In the plateau area (40–50 mm) approximately (57–59)%, (59–63)%, (52–63)% and (58–61)% of the overall absorbed-EAIE was due to scattered and reabsorbed radiation for the LSO, GSO, YAP and LuAP scintillators, respectively.

Scatter to primary ratio (SPR) presented variations between the various scintillators. The curves are not presented for brevity. For the LSO and GSO scintillators the SPR was found to be 53.3% and 59.0% at the 10 mm thickness and 62.1% and 68.2% at the 50 mm thickness, respectively. For the YAP and LuAP scintillators these values were 91.8% and 55.0% at the 10 mm thickness, and 92.7% and 63.5% at the 50 mm thickness, respectively.

At the thickness range above 10 mm and for all the investigated scintillators, a negligible part—below 0.1%—of the generated fluorescence radiation, was found to be transmitted through the scintillator block. This implies that, all the generated fluorescence radiation is finally absorbed within each scintillator block. In addition, the fraction of the overall absorbed-EAIE corresponding to the absorption of the generated fluorescence radiation within the scintillating crystal presents variations between the four studied scintillators. Specifically, for the LSO scintillator this fraction—over total—had the value of 12.1% at the 10 mm thickness and 62% at the 50 mm thickness. For the GSO scintillator these values were 5.1% and 35.2%, respectively. For the YAP and LuAP scintillators these values were found to be 0.1% and 2.61% and 2.61% and 13.8%, respectively. In the whole thickness range studied and for all the investigated scintillators, the fractions of the reabsorbed generated fluorescence radiation corresponding to L- and lower shell fluorescence characteristic photons, were significantly lower than those above this K-edge. These results indicate that the contribution of the fluorescence radiation to the overall absorbed-EAIE is mainly due to *K*-characteristic photons. Similar results are also reported by others in the X-ray energy range [16,17]. These issues indicate also that, above *K*-edge, a significant part of the overall absorbed-EAIE is due to reabsorption of *K*-characteristic fluorescence radiation. Similar results reported by others were in close agreement [9,16–19].

Fig. 3 presents the variation of QDE with thickness for the four scintillators under study. For the LSO, GSO, YAP and LuAP scintillators QDE was found to be 54.9%, 48.8%, 37.4% and 56.8% at the 10 mm thickness and 96.4%, 95.4%, 89.9% and 96.9% at the 50 mm thickness, respectively. The shapes of the QDE curves presented

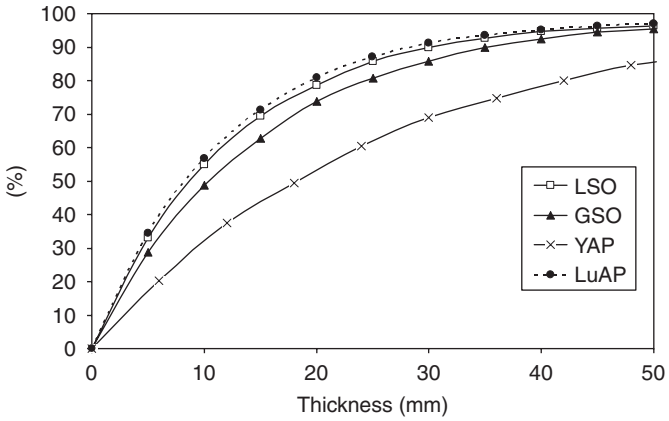

Fig. 3. QDE at 511 keV for the four scintillators under study.

similarities to the corresponding curves of the overall absorbed-EAIE but they are shifted up to higher values. This was more strongly observed for the YAP scintillator. The up-shift of the QDE values in respect to the corresponding ones of the overall absorbed-EAIE could be explained on the basis of the determination of these two efficiency metrics. QDE values are higher, since a photon can be detected; however, without its energy being totally absorbed by the absorbing medium, e.g. escaping the medium after having undergone one or more Compton and coherent scatterings.

QAE presented similar curve shapes with thickness to those of the overall absorbed-EAIE. These are also not shown for brevity. For the LSO, GSO, YAP and LuAP scintillators QAE was found to be 20.6%, 32.3%, 10.1% and 41.1% at the 10 mm thickness and 93.8%, 92.5%, 54.6% and 94.3% at the 50 mm thickness, respectively.

Fig. 4 presents the variation of QAE-PA with thickness for the four scintillators under study. For the LSO, GSO, YAP and LuAP scintillators QDE-PA was found to be 17.7%, 13.2%, 1.5% and 16.7% at the 10 mm thickness and 29.8%, 24.1%, 3.8% and 27.6% at the 50 mm thickness, respectively. The higher values of the LSO and LuAP scintillators are indicative of their high chance of detection due to photoelectric effect as also reported by others [1].

In comparison, for the scintillators under study and regarding their detection efficiency, the LSO and LuAP scintillators presented higher detection efficiency values using either energy or quantum efficiency metrics, i.e. overall absorbed-EAIE, QDE and QAE. On the other hand, GSO scintillator presented comparable overall absorbed-EAIE, QDE and QAE values, especially for thick crystals, i.e. above 20 mm. The YAP scintillator was found to be of lesser importance, except if very thick crystals are considered. For example, the overall absorbed-EAIE of a 40-mmthick YAP crystal is comparable to a 10 mm LSO or LuAP one.

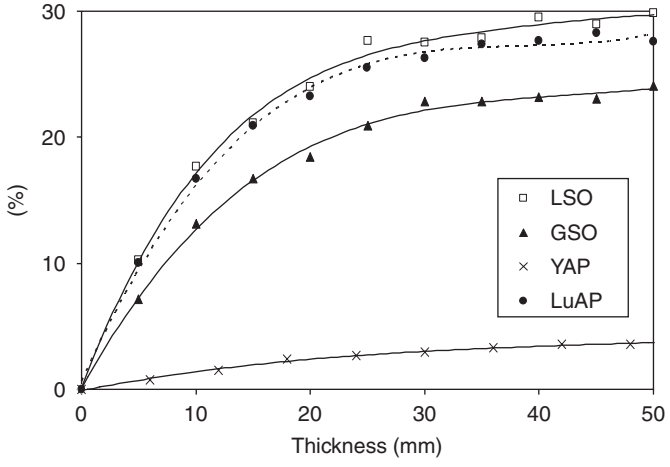

Fig. 4. QAE-PA at 511 keV for the four scintillators under study.

In investigating the role of scattering—mainly Compton—it is interesting to note that the YAP scintillator presented the lowest scatter and reabsorbed-EAIE in the whole thickness range, while simultaneously presented the highest SPR values. This behaviour of the YAP crystal makes it optimal for small-animal PET systems were Compton events due to scattering within the scintillator are acceptable [1]. On the other hand, LSO and LuAP presented less SPR and higher scatter and reabsorbed-EAIE in the whole thickness range; this makes them more optimal for other PET applications, since more efficient photopeak–windowing and better true to random coincidence ratio may be achieved [1].

In conclusion, the LSO and LuAP scintillators may be considered better for PET imaging compared to GSO and YAP, but their high cost [1] constrains their application. Nevertheless, their higher light yield and their shorter response time [1]—compared to BGO—makes them very interesting candidates to replace BGO. GSO is a scintillator compensating cost and efficient detection, however, it is constrained by the difficulty in growing large crystals [1]. On the other hand, YAP may be considered adequate only for small-animal PET systems.

Acknowledgments

This work was financially supported by the Greek Ministry of Education (program EPEAEK ‘Archimidis’).

References

[1] C.W.E. van Eijk, Phys. Med. Biol. 47 (2002) R85.
[2] D.W. Townsend, Proceedings of the Sixth International Conference on Inorganic Scintillators and thir use in Scientific and Industrial Appications SCINT 2001, IEEE Trans. Nucl. Sci. NS-36 (2001) 1056.
[3] K. Wienhard, M. Dahlbom, L. Eriksson, T. Bruckbauer, U. Pietrzyk, w.d. Heiss, IEEE NSS/MIC Conference Record CDROM 17 (2000) 2.
[4] P. Lecop, Proceedings of the Sixth International Conference on Inorganic Scintillators and their use in Scientific and Industrial Applications SCINT 2001.
[5] J.J.S. Karp, S. Surti, M.E. Daube-Witherspoon, R. Freifelder, C.A. Cardi, L.E. Adam, K. Bilger, G. Muehllehner, J. Nucl. Med. 44 (2003) 1340.
[6] Del Guerra, M.G. Bisogni, C. Damiani, G. Di Domenico, R. Marchesini, G. Zabattini, Nucl. Instr. Meth. Phys. Res. A 442 (1–3) (2000) 18.
[7] S. Weber, A. Bauer, H. Herzog, F. Kehren, H. Muehlenseipen, J. Vogelbruch, H.H. Coennen, K. Zilles, H. Halling, IEEE Trans. Nucl. Sci. NS-47 (2000) 1665.
[8] I. Valais, I. Kandarakis, D. Nikolopoulos, I. Siannoudis, N. Dimitropoulos, D. Cavouras, C.D. Nomicos, G.S. Panayiotakis, IEEE Trans. Nucl. Sci. NS-52 (5) (2005) 1830.
[9] H.P. Chan, K. Doi, Phys. Med. Biol. 28 (5) (1983) 565.
[10] H.P. Chan, K. Doi, Med. Phys. 12 (2) (1985) 153.
[11] J.H. Hubbel, S.M. Seltzer, Tables of X-ray mass attenuation coefficients and mass energy absorption coefficients 1 keV to 20 MeV for elements $Z = 1$–92 and 48 additional substances of dosimetric interest. US Department of Commerce. NISTIR 5632, 1995
[12] ftp://physics.nist.gov/PhysRefData/.
[13] ftp://ftp://www-phys.llnl.gov/pub/rayleigh/RTAB/data_NF/.

[14] J.M. Boone, J.A. Seibert, J.M. Sabol, M. Tecotzky, Med. Phys. 26 (6) (1999) 905.
[15] I. Kandarakis, D. Cavouras, Eur. Radiol. 11 (2001) 1083.
[16] J.M. Bonne, V.N. Cooper, Med. Phys. 27 (8) (2000) 1818.
[17] J.M. Boone, X-ray production, interaction, and detection in diagnostic imaging, in: J. Beutel, H.L. Kundel, R.L. Van Metter (Eds.), Handbook of Medical Imaging, Physics and Psycophysics, vol. 1, SPIE Press, Bellingham, 2000, p. 40.
[18] I. Kandarakis, D. Cavouras, E. Ventouras, C. Nonicos, Rad. Phys. Chem. 66 (2003) 257.
[19] H.W. Vanema, Radiology 130 (1979) 765.